



# Modelling Holocene stratigraphy and depocentre migration of the Volga delta due to Caspian Sea-level change

I. Overeem<sup>a,\*</sup>, A. Veldkamp<sup>b</sup>, L. Tebbens<sup>c</sup>, S.B. Kroonenberg<sup>d</sup>

<sup>a</sup>*Institute of Arctic and Alpine Research, University of Colorado, 1560 30th Street, Boulder, CO 80309-0450, USA*

<sup>b</sup>*Department of Soil Science and Geology, Wageningen University, Wageningen, The Netherlands*

<sup>c</sup>*Department of Physical Geography, Utrecht University, Utrecht, The Netherlands*

<sup>d</sup>*Faculty of Applied Earth Sciences, Delft University of Technology, Delft, The Netherlands*

Received 30 August 2001; accepted 28 May 2002

## Abstract

The Volga system is sensitive to allogenic control due to its low on- and offshore gradient ( $\sim 5$  cm/km). In sequence stratigraphy, little attention has been paid to the effects of sea-level change in these ramp-margin fluvio-deltaic settings. The high-frequency sea-level changes of the Caspian basin have considerable amplitude (up to 18 m) over the Holocene time-span, which is usually considered as the lower boundary of fifth-order cycles.

A process–response model, AQUATELLUS, has been used to investigate fluvio-deltaic response to sea-level fluctuation. Calibration of the model with measured data over the last century, comprising a full 3-m sea-level cycle, showed plausible progradation and sedimentation rates.

The numerical modelling showed that sea-level changes forced the Holocene Volga delta to migrate  $\sim 200$  km over the Caspian plain, leaving only thin laterally extensive deposits. The frequent depocentre shifts add a whole new perspective to the ongoing discussion about the impact of sea-level changes along the longitudinal profile.

The periods during which significant deposition occurred coincide with the times that migration distances were relatively low. Thicker progradational wedges have been deposited at these time intervals, at  $\sim 9000$ – $8000$ ,  $\sim 7400$ – $6700$ ,  $\sim 5200$ – $3700$  and  $\sim 2400$ – $900$  years BP.  $^{14}\text{C}$  dated deposits in the lower delta plain area corroborate the model output. Remarkably, this is both in highstand and lowstand conditions.

The low gradient makes wave effects insignificant and tides are nonexistent, so that the fluvial deposits are hardly reworked and no shoreface facies or maximum flooding surface develop.

The Volga delta response indicates that sequence-stratigraphic concepts are not scale-independent in low-gradient settings and that short-term high-frequency sea-level changes have a far-reaching impact on the stratigraphy.

© 2002 Elsevier Science B.V. All rights reserved.

*Keywords:* Volga delta; Holocene; Numerical modelling; Sequence stratigraphy

\* Corresponding author. Tel.: +1-303-492-6631; fax: +1-303-492-3287.

E-mail address: [irina.overeem@colorado.edu](mailto:irina.overeem@colorado.edu) (I. Overeem).

## 1. Introduction

### 1.1. Theoretical sequence-stratigraphic framework

Sedimentation and erosion patterns in fluvio-deltaic systems are controlled by many different factors, such as tectonic setting, nature of the source area, nature of the basin, sediment grain size, climate, and sea level (Coleman and Wright, 1975; Orton and Reading, 1993). The complexity of the response of the fluvial system to sea-level changes (Posamentier and Vail, 1988) and the importance of incorporation of other controls such as tectonics and climate into the sequence-stratigraphic framework has been realized over the last decade (Miall, 1991, 1996; Schumm, 1993; Shanley and McCabe, 1994; Blum and Törnqvist, 2000). Unravelling the effects of each of these factors can best be accomplished in systems that show a strong dominance of one factor over the others (Schumm, 1991).

In this paper, we will demonstrate the effect of sea-level change as a unique dominating factor on a prominently, fluvially controlled delta, the Volga delta in the Caspian Sea. This delta differs from most other large deltas in the world in two aspects. Firstly, it has an extremely gentle onshore and offshore gradient of 5 cm/km extending over 200 km into the basin, so it can be classified as a ramp margin. Secondly, it is subject to extremely rapid changes in base level, because the Caspian Sea is a closed basin with a very dynamic sea-level regime independent of that of the oceans (Kroonenberg et al., 1997, 2000a; Overeem et al., *this issue*; see these papers for geological setting). During the Holocene, several significant (meter-scale) fluctuations have occurred, although the sea level never dropped below the shelf edge. These sea-level fluctuations are of even higher frequency than a fifth-order cycle, defined to be of  $10^4$  years duration (Vail et al., 1977).

The stable tectonic situation of the Volga delta on the border of the Eurasian Platform and the absence of tides and limited wave action (Overeem et al., *this issue*) make it an ideal case to study the impact of high-frequency sea-level change on a fluvial–deltaic system without interference of tectonic and interacting marine factors.

### 1.2. Study setup and objectives

We have studied the impact of high-frequency sea-level changes on the Volga system in two different ways. A field study was carried out to understand the impact of sea-level change on stratigraphy in the recent and Holocene Volga delta. The combination of low-gradient and rapid sea-level changes leads to extremely rapid lateral and vertical facies shifts on small spatial scales, which are difficult to interpret in the classical sequence-stratigraphic framework. This is reported in an accompanying paper (Overeem et al., *this issue*).

Here, we report the results of numerical modelling of the evolution of the Volga delta. Numerical modelling is a powerful tool to ‘understand the nature of geological processes by examining the range of possible relationships under a variety of assumptions’ (Howes and Anderson, 1988). It forces us, scientists, to formulate hypotheses in a quantitative way (Cross, 1989; Paola, 2000). Furthermore, it provides the opportunity to integrate controlling processes, whereby the internal forcing may induce unanticipated system response (Watney et al., 1999). As such, modelling is used here to gain quantitative insight in the role of sea-level changes and slope characteristics on stratigraphy and depocentre migration over a intermediate time-scale ( $10^4$  years).

## 2. Model engine: process descriptions of sediment transport along a longitudinal profile

A 2-D process–response model, AQUATELLUS, has been designed that integrates fluvio-deltaic process descriptions for large spatial and temporal scales. Over large (geological) time scales, major floods and storms are the relevant transport events. A large spatial scale is chosen and a typical longitudinal profile extends over 10–100’s of kilometres. This still is an order of magnitude smaller than classical basin models (e.g. Steckler et al., 1993; Flemings and Grotzinger, 1996). The chosen macroscopic scale requires simplification of process descriptions while on the other hand the dynamic nature of the processes requires a certain degree of freedom. The essence of the approach is integration of a mass balance that transforms spatial differences in sediment transport to

rates of erosion or deposition over time. The sediment transport rates respond dynamically to changes in topography and depositional environment as a continuity equation (modified after Kirkby, 1992; Veldkamp and van Dijke, 1998, 2000; Tebbens et al., 2000; Storms et al., 2002). We model the system as a semiclosed system. A longitudinal profile is seen as a ‘hose’ that transports incoming sediment downstream. The lower boundary condition for sediment flux is undefined.

$$\frac{\partial H_x}{\partial t_x} = \frac{\partial F}{\partial x} + T \quad (1)$$

The upper boundary conditions are specified as input (see under model input):

$$H_{(x,0)} = f(x) \text{ specifies an initial profile}$$

for each case study;

$$F_{(0,t)} = g(t) \text{ specifies variability in incoming}$$

flux over time

where:  $H$  = topographical height [L];  $t$  = time [T];  $F$  = sediment flux [ $L^2 T^{-1}$ ];  $T$  = rate of vertical tectonic movement [ $L T^{-1}$ ];  $x$  = horizontal distance [L].

The sediment flux gradient, which is the spatial derivative of the sediment flux, is described as the resultant of the erosion and sedimentation fluxes (Eq. (2), Fig. 1). Erosion flux (Eq. (3)) and sedimentation flux (Eq. (5)) are described conceptually different, which is the main conceptual difference to diffusion-based models (e.g. Rivenaes, 1992; den Bezemer, 1998).

$$\frac{\partial F_x}{\partial x} = \frac{\partial F_{\text{ero}(x)}}{\partial x} - \frac{\partial F_{\text{sed}(x)}}{\partial x} \quad (2)$$

where:  $F_{\text{ero}}$  = erosion flux [ $L^2 T^{-1}$ ];  $F_{\text{sed}}$  = sedimentation flux [ $L^2 T^{-1}$ ]. The erosion flux depends on the stream power, which is determined by discharge and local slope. This approach has been used by Tucker and Slingerland (1994) and Kooi and Beaumont (1996) for the upper reach of river systems, where erosion is the dominant process.

$$\frac{\partial F_{\text{ero}}}{\partial x} = k S^m Q(x)_t \quad (3)$$

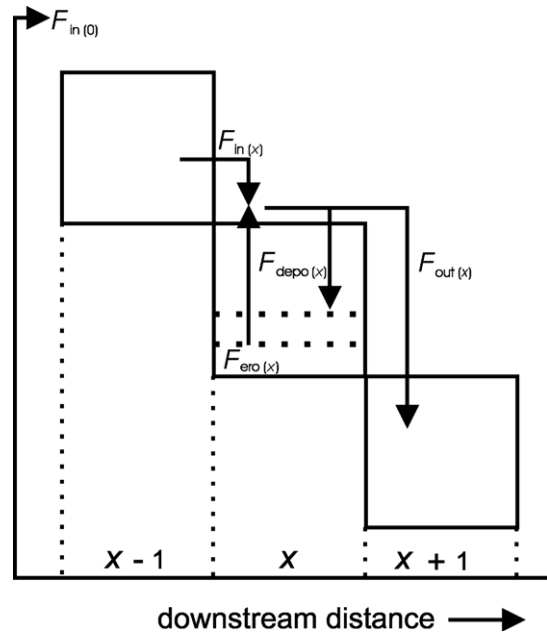


Fig. 1. Schematic representation of the sediment fluxes for a single grid cell along the longitudinal profile.

where:  $Q(x)$  = discharge function [ $L^2 T^{-1}$ ];  $S$  = slope [ $L L^{-1}$ ];  $m$  = constant [-];  $k$  = erosion efficiency [ $L^{-1}$ ].

The discharge function  $Q(x)$  differs for fluvial and marine environments. In the fluvial domain, discharge increases downstream, reflecting an increasing contributing drainage area. Offshore,  $Q(x)$  decreases with increasing water depth, mimicking the effect of decreasing fluvial influence in the marine basin due to lateral spreading of the deltaic plume (Albertson et al., 1950; Wright, 1977; Nemeč, 1995; Morehead and Syvitski, 1999). The constant  $m$  is chosen equal to 1 in the fluvial domain, to obtain a linear slope-dependent relation. In the marine domain,  $m$  is set to be equal to 0, making erosion essentially slope-independent. Erosion due to wave action is not incorporated. We consider these assumptions valid for the specific low-gradient setting, and because we do not model the shelf edge.

The erosion constant,  $k$ , is the local efficiency of the system to erode sediment. In the fluvial and marine domains, different values for the erosion constant,  $k$ , are used, because the erosion efficiency varies significantly between confined and unconfined flows

and with varying oceanographic influences. It is possible to incorporate differences in the cohesion of the substrate, by differing  $k$ , (Tebbens et al., 2000), but this has been omitted in our model.

Erosion is modelled as a grain-size independent process. The large temporal scale justifies this simplification, because peak floods will then be the significant erosional events, which are capable of eroding all simulated grain-size classes.

*Sedimentation* is defined as a first-order kinetic reaction (as often used in concentration problems), implying that the sedimentation ( $F_{\text{sed}}$ ) is proportional to the sediment load of the water ( $F$ ). This flux of sediment in transit is the sum of the local erosional flux ( $F_{\text{ero}}$ ) and the incoming sediment load ( $F_{\text{in}}$ ). The outflux ( $F_{\text{out}}$ ) is the sediment left in concentration, which travels further downstream (Fig. 1).

$$F = F_{\text{in}} + F_{\text{ero}} = F_{\text{sed}} + F_{\text{out}} \quad (4)$$

$$\frac{\partial F_{\text{sed}}}{\partial x} = \frac{F_{(x,t)}}{h} \quad (5)$$

where:  $F_{(x,t)}$  = absolute sediment flux [ $\text{L}^2 \text{T}^{-1}$ ];  
 $h$  = travel distance [L].

The solution to Eq. (5) forces one to have an exponential fallout. The inverse of the travel distance,  $h^{-1}$ , can be seen as proportional to the probability of deposition along the transport pathway. The travel distance is set to be dependent on both grain size, implying that coarse sediment has a steep curve and limited travel distance, whereas fine sediment has a gentle curve and travels far along the profile. Furthermore, it is dependent of the environment. The settle rate at entering the marine basin is initially high due to a loss of momentum and subsequently decreases exponentially with distance from the river-mouth (e.g. Kaufman et al., 1992; Bursik, 1995).

Offshore, the sediment flux is manipulated to reflect the lateral spreading of the fluvial plume. We need to incorporate this aspect, because we model a 2-D profile and just follow the plume axis.

$$F_{\text{sed}(x,t)} = F_{\text{sed}(x-1,t)} - (F_{\text{sed}(x-1,t)} 2D_{\text{coast}} \tan\alpha) \quad (6)$$

where:  $D_{\text{coast}}$  = distance from the coastline [m];  $\alpha$  =  $20^\circ$ , typical for bedfriction-dominated plumes (Wright, 1977).

### 3. Model input

#### 3.1. Initial profile

Ideally, the longitudinal profile of the Volga River from the apex onwards and its delta at the beginning of the Holocene has to be provided as model input (Table 1). As there are no explicit topographical data, the following rationale is used. Ohmori (1991) states that the longitudinal profiles of rivers with well-developed levee and delta systems are best described by exponential functions. The deltaic plain from the apex onwards can then be considered to be the tail of the exponential curve, being an approximately linear function. The North Caspian Basin was tectonically rather stable over the Holocene (Kvasov, 1987), which is confirmed by geodetic measurements over the last century (Lilienberg, 1995). Consequently, the present delta gradient of 5 cm/km, (Kroonenberg et al., 1997) is probably approximately representative. In the lower delta plain area, a paleogradient of 8 cm/km has been reconstructed (Overeem et al., this issue), which is in the same order of magnitude.

#### 3.2. Discharge and sediment input

Time-continuous data on paleodischarges ( $Q$ ) and sediment load ( $Q_s$ ) of the Volga River in the Holocene are not available. Caspian Sea level (CSL) is strongly influenced by climatic fluctuation in the Volga drainage basin (Maev, 1993 in Rychagov, 1997). There is a strong feedback between Volga discharge and CSL (Fig. 2). Most of the Volga discharge (about 78%) originates from north of latitude  $50^\circ\text{N}$ . For this reason, the sea surface temperature in the Barents Sea area has been found to be a statistically significant predictor for long-term variations in the CSL (Rodionov, 1994). This conclusion and continental pollen data (Khotinskiy, 1984; Kremenetski et al., 1999) support the assumption that we can use temperature as an important climate parameter influencing the runoff of the Volga River. Therefore, we follow the approach advocated by Tebbens et al. (2000) to use temperature changes inferred from  $\delta^{18}\text{O}$  data as a proxy for Holocene discharge variation.  $\delta^{18}\text{O}$  data derived from the Greenland Ice Sheet Project 2 (GISP) core (Fig. 3, Stuiver et al., 1995) are used as a relative measure for temperature changes in the Northern Hemisphere over

Table 1  
Simulation parameters for both the calibration and the actual simulation

Simulation parameters	1900–1990 calibration run	Holocene
<i>Time scenario</i>		
Total simulation time (years)	90 (period 1900–1990)	10,000
Time step (years)	1	10
<i>Grid dimensions</i>		
Length of longitudinal profile (grid cells)	500	500
Grid cell length (m)	1000	1000
<i>Sea-level scenario</i>		
Sea level at $t=0$ (m)	from file, last century sea level	from file, Rychagov, 1997
Sea level amplitude (m)	from file, last century sea level	from file, Rychagov, 1997
<i>Initial profile</i>		
Slope (m/km)	0.07	0.07
<i>Discharge and sediment load</i>		
$Q$ at $t=0$ ( $m^3/s$ )	1830	2090
$Q_s$ at $t=0$ ( $m^3/s$ )	40	4
$Q$ variation range in time	last century range (1.54–0.62)	fluctuation acc. $\delta^{18}O$ range idem as calibration
$Q_s$ variation range in time	last century range (1.53–0.59)	fluctuation acc. $\delta^{18}O$ , range idem as calibration
<i>Grain-size characteristics</i>		
Number of grain-size classes	6	idem
Percentage distribution	0.2, 0.2, 0.2, 0.2, 0.1, 0.1	idem
Grain sizes (mm)	0.0044, 0.088, 0.177, 0.23, 0.35, 0.5	idem
<i>Sediment transport coefficients</i>		
Travel distances fluvial domain (m)	50,000, 40,000, 30,000, 12,000, 8000, 4000	idem
Travel distances marine domain (m)	7000, 6000, 5000, 4000, 1000, 200	idem
Erosion capacity fluvial domain ( $m^{-1}$ )	0.005	idem

Table 1 (continued)

Simulation parameters	1900–1990 calibration run	Holocene
<i>Sediment transport coefficients</i>		
Erosion capacity marine domain ( $m^{-1}$ )	0.000005	idem
Spreading angle plume ( $^{\circ}$ )	20 (bedfriction)	idem

the Holocene. The data consist of a continuous record of 20-year averages of  $\delta^{18}O$  isotopes.

For the purpose of our model, the isotope data were normalised to form a *relative climate factor*. This factor forces the discharge and sediment load to change in time (Fig. 3). A random noise factor is used to interpolate to 10 years time resolution, which is used in the modelling to acknowledge at least some of the natural variability and complex response to temperature changes.

To obtain absolute discharge and sediment load values, a link to present-day discharges is made. Discharge at the river mouth is currently  $\sim 8400 m^3/s$  (Polonski et al., 1998) and the average over 1888–1980 is  $7835 m^3/s$  according to Kosarev and Yablonskaya (1994). This discharge is distributed over four main zones, of which we model only a single one, so the input for the model is about  $2000 m^3/s$ . The measured highest and lowest yearly flows over the last hundred years indicate a range of 1.54–0.62 (Rodionov, 1994; Polonski et al., 1998). To keep to the conservative side, this range is chosen for the Holocene. The resulting variation in discharge after multiplication with the relative climate factor is  $3080$  to  $1240 m^3/s$  over the Holocene.

Clearly, this may be an underestimation of sediment and erosion rates because peak events on a 100–1000-year time scale are recognized in many studies to have far-reaching influence (Roberts, 1998; Syvitski and Morehead, 1999; Sommerfield and Nittrouer, 1999; Imran and Syvitski, 2000). However, these studies specifically emphasize increased erosion and across shelf transport, whereas the Volga system is very unconfined in case of peak floods, basically increasing the floodplain sedimentation rates (Belevich, 1960).

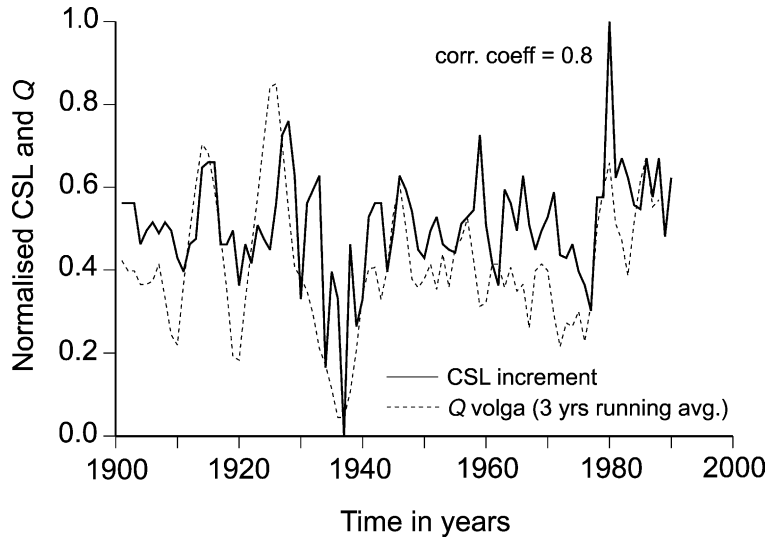


Fig. 2. Measured data over the last century (1900–1990) are used as input for constraining the model. Volga River discharge ( $\text{km}^3/\text{year}$ ) and Caspian Sea level (CSL) over the last century (after Kosarev and Yablonskaya, 1994). Data show that the 3 years running average of the Volga discharge and the CSL increments are positively correlated.

Sediment load estimates vary from  $0.097$  (Kosarev and Yablonskaya, 1994) to  $0.2317 \text{ m}^3/\text{s}$  (Lisitzin, 1972). If one estimates the load on the basis of drainage area (cf. Milliman and Syvitski, 1992), it is calculated to be  $0.171 \text{ m}^3/\text{s}$ . Polonski et al. (1998) show a roughly linear relation between the discharges and corresponding sediment load as yearly averages over specific periods (1950–1955, 1956–1960, 1961–1970, 1971–1977 and 1978–1993). This relation justifies the assumption that  $Q$  and  $Q_s$  in the model vary according to the same relative climate

factor. Relative fluctuations of the sediment load measured from 1950 onwards in the peak month May are in a similar range as discharge variations,  $1.53$ – $0.59$  (Polonski et al., 1998), so that multiplication with the relative climate factor appears to yield a reasonable range.

### 3.3. Sea level

Sea-level data are straightforward, based on the independent sea-level curve of Rychagov (1993,

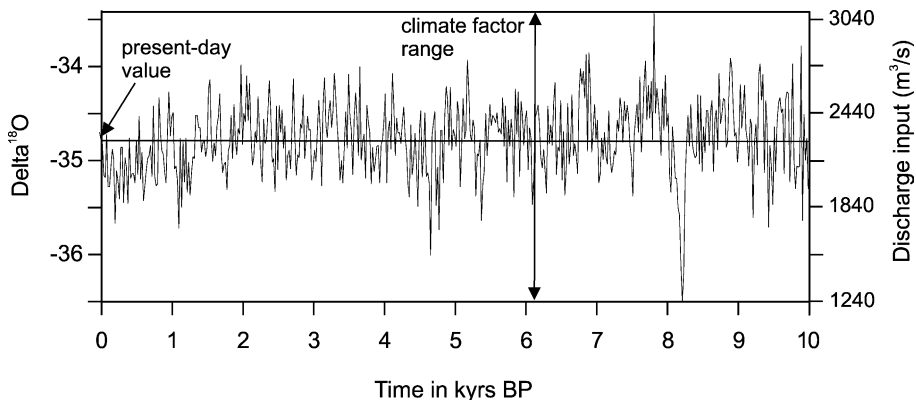


Fig. 3. Climatic fluctuation over the Holocene based on ice core data of GISP-core 20-year  $\delta^{18}\text{O}$  record (Stuiver et al., 1995, on the left axis) determines the *relative climate factor*. This factor is used to force fluctuation in discharge (on right axis) in time.

1997) (Fig. 4 in accompanying paper of Overeem et al., this issue). That curve has been reconstructed based on terrace heights at the Dagestan coast, to the south in the Caspian Basin, which implies that the highstand sea levels have been determined with much greater accuracy than the lowstand sea levels. The validity of the curve is discussed in Kroonenberg et al. (1997). To overcome any data gaps, the curve has been splined to obtain a time-continuous input.

### 3.4. Grain-size parameters

The grain-size distribution of recent Volga delta sediments (uppermost 1.2 m) based on 120 samples shows (Fig. 4) a large peak of well-sorted fine sands (50–150  $\mu\text{m}$ ) and less well-sorted clays (median at approximately 4  $\mu\text{m}$ ). These data have been used to determine an estimate for the model input. Six grain-size classes, with emphasis on the fines, have been used during modelling with their medians at 0.0044, 0.088, 0.177, 0.23, 0.35 and 0.5 mm, respectively.

Subsequently, travel distances,  $h$ , for each of the grain-size classes had to be estimated. There are no

explicit data on this parameter. It is clear that in the fluvial system the capacity to bypass sediment is much larger than in the marine domain, so that travel distances are an order of magnitude larger in the fluvial domain. Tebbens et al. (2000) estimated the bulk sediment travel distance for the Meuse system based on the extent of the coarsest-grained fluvial wedge to be 80 km. In the Volga system, the gravels and most coarse sands are settling mainly upstream, making the bulk travel distances in the fluvio-deltaic domain probably a lot higher.

In the marine domain, the remaining coarse sands will be deposited in mouth bars rather close to the shoreline. However, surface samples of sediment from our fieldwork show no significant fining trend in the first 10 km offshore (Overeem et al., this issue, accompanying paper). Satellite and aerial photographs show that a suspension plume of the Volga River extends over 75 km offshore during fair-weather conditions (Kroonenberg et al., 1997). We inferred that in the marine domain the travel distances have to be at least in an order of magnitude of  $10^2$ – $10^4$  m. It is clear that the data available to determine the grain-size parameters in the model are of qualitative value, which makes calibration of these parameters necessary.

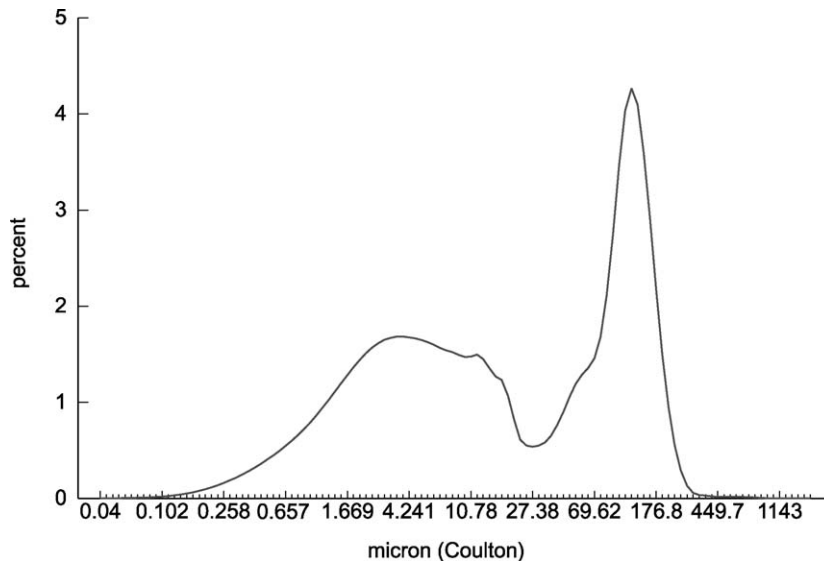


Fig. 4. Average grain-size distribution of recent Volga delta sediment, based on Coulton laser analysis of 120 shallow augering samples (within first 1.2 m). A distinct peak at the clay fraction, and for the silt—fine-sand fraction has been observed. The samples contained remarkably little coarse sands.

#### 4. Model calibration

The common calibration procedures for process–response models are extensively discussed in [Tebbens and Veldkamp \(2000\)](#). We calibrated the model to last century data (1900–1990), comprising a full sea-level cycle. The input parameters are listed in [Table 1](#). Discharge of the Volga,  $Q$  and CSL have been measured over this time span ([Kosarev and Yablonskaya, 1994](#); [Rodionov, 1994, Fig. 2](#)). Two criteria are used to judge the reliability of the model, both of which can be easily compared with model output. On

one hand, depocentre migration, on the other hand, net sedimentation.

Aerial photographs of the Damchik area since 1935 have been used to study depocentre migration during the last 3 m sea-level cycle ([Lychagin et al., 1995](#); [Labutina et al., 1995](#); [Baldina et al., 1999](#); [Kroonenberg et al., 2000b](#); [Overeem et al., this issue](#)). Based on this analysis, the ‘normative’ progradation during calibration for the last sea-level fall was 25 km for roughly the period 1930–1950. Between 1950 and 1977, further sea-level fall did only result in about 500 m progradation, although the passive emergence of

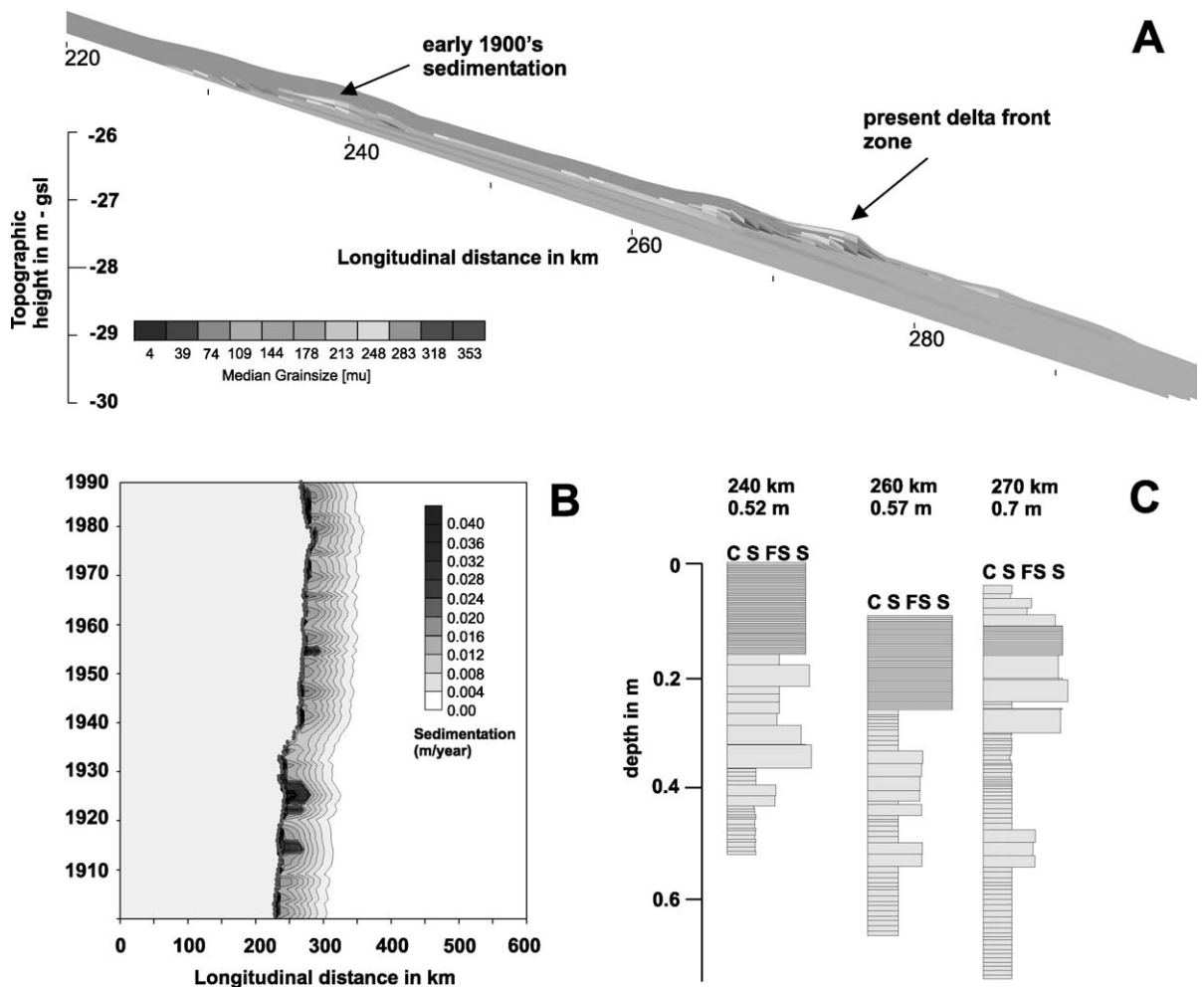


Fig. 5. Simulation results of calibration run from 1900 to 1990 for the Volga delta. (A) Stratigraphic longitudinal profile. (B) Profile evolution model, the  $x$ -axis shows the distance at the longitudinal profile, while the  $y$ -axis shows the time. Dark colors indicate the high sedimentation areas, generally the active delta. (C) Simulated augerings (C=clay, S=silt, FS=fine sand, S=sand).



reedlands added to the coastline progradation. The subsequent sea-level rise between 1977 and 1995 resulted mostly in aggradation, the depocentre position basically remained stable.

Augerings showed an average net sedimentation of  $1.1 \pm 0.4$  m for the delta sediments, deposited during the recent 3-m sea-level cycle, which could be clearly distinguished in the field (Overeem et al., this issue). This amounts to a rate of  $1.1 \text{ m}/65 \text{ years} = 1.7 \text{ cm/year}$ , which is comparable to sedimentation rates inferred from  $^{137}\text{Cs}$  datings (Winkels et al., 1996). This number is an overestimation because augerings have been taken in many cases on active levees. To overcome this bias, we decided that the model should

show a response comparable to the lower boundary of values encountered in the augerings; 0.7 m. Nonetheless, the actual average Holocene sedimentation rate is again an order of magnitude lower as roughly estimated from  $^{14}\text{C}$  datings; in the order of 1.3 mm/year (Overeem et al., this issue). The thickness of the sediment layer above the Pleistocene base averaged over the augerings in the study area was 5.5 m, which gives approximately 0.6 mm/year.

Many simulations with input parameters of the last century have been run, until we considered the results plausible and matching the criteria obtained from the field data. Model results are depicted in Fig. 5A–C. Here not only net sedimentation in each time step is

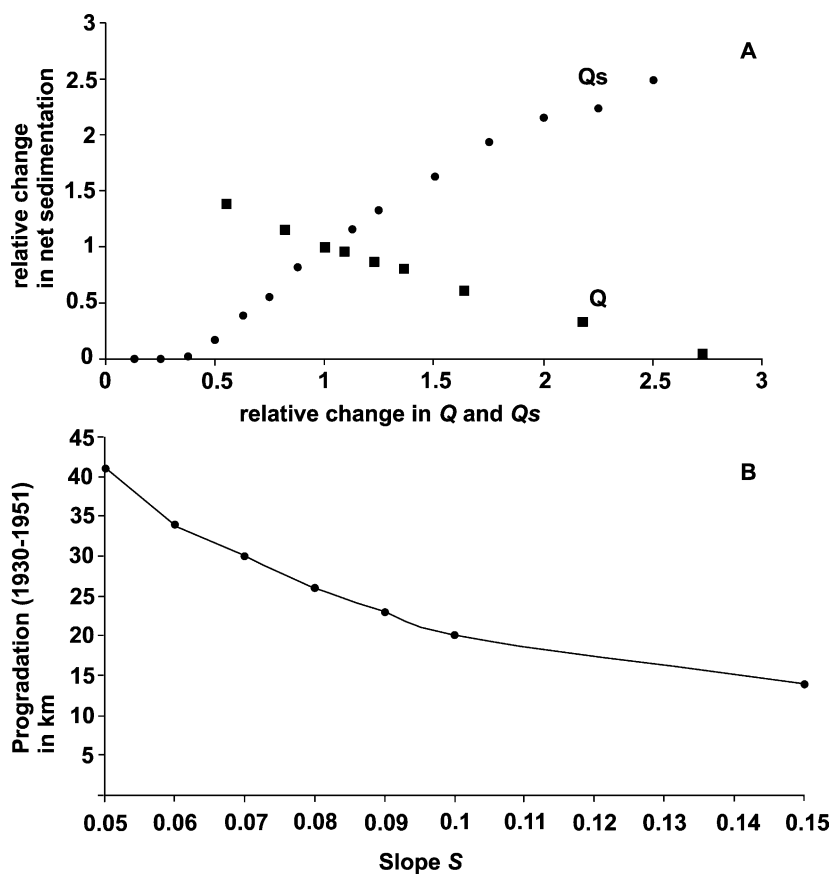


Fig. 6. Sensitivity experiments of the calibration run. (A) Relative changes in  $Q$  and  $Q_s$  strongly influence the net sedimentation rate over the last century. Simulated net sedimentation proved to be more sensitive to initial sediment load variation than to discharge. (B) Progradation of the coastline depends on the slope that is initially set. The range of slopes under which reasonably accurate progradation rates are modelled is rather wide.

visualised, but also the total resulting stratigraphy, including grain size, visualised as the median of the grain-size distribution. The stratigraphic profile of the last century shows initially delta front sedimentation at about grid cell 240, which rapidly progrades to 260–270 and remains basically stable for a longer period, prograding only slowly to about 280. A profile evolution model (Fig. 5B) shows the net sedimentation over a longitudinal profile (on the  $x$ -axis) in time ( $y$ -axis) (cf. Wheeler diagrams). The bright line indicates the simulated coastline position. It can be seen that the most rapid progradation occurred at the period of rapid sea-level fall between 1930 and 1940. Besides that, the importance of fluctuation of the discharge and sediment load can be seen from the yearly fluctuation of the extent of the deltaic plume. It is to some extent influenced by the discharge- and sediment-peak years.

A general coarsening upwards trend results from the progradation, which is evident in the simulated augering (Fig. 5C). The rising of the sea level seems to affect the present near-coastal zone, where a veneer of fine material has been deposited lately (Fig. 5A,C). In the simulated augering at grid cell 270, these deposits form a thin fining-upward layer. This drowning of the delta is corroborated by field observations of clay and silt layers on top of fine-sandy levees and mouth bars (Overeem et al., *this issue*).

Over the 90 years simulation period, the total net sedimentation varied from 0.58 m immediately upstream of the area of the early century coastline (at grid cell 240) to 0.75 m close to the present coastline (at grid cell 270). This is within the range of sedimentation rates retrieved from field data over the last century. An order of magnitude reduction of sediment load is necessary to obtain reasonable sedimentation rates over the Holocene. This is an exact reflection of the perception based on the field data that sedimentation rates are different for the different time scales. Naturally, the discrepancy can be attributed to lateral dynamics, because lobes and channels spread sediment over larger lateral zones as the time scale increases.

The generated output under the set input conditions seemed to make geological sense. In addition, to verify the robustness of our model, we varied the input parameters;  $Q$ ,  $Q_s$  and slope,  $S$ . It can be seen that net sedimentation at the coastline is more sensitive for relative changes in the initial load than for changes in

the input discharge (Fig. 6A). This implies that especially initial sediment input has to be carefully chosen.

We identified initial slope as another important control. Simulations show that the initial slope does influence the simulated progradation (Fig. 6B), but the range of slopes which still gives plausible progradation distances is wide enough to be fairly confident of the assumed slope of 7 cm/km.

## 5. Model output: simulated deltaic response over the Holocene

### 5.1. Depositional patterns

A profile evolution model shows the net sedimentation over a longitudinal profile in time (Fig. 7). The model simulates the net sedimentation over an along-stream distance of 500 km in the Volga delta plain in time steps of 10 years. Fig. 7 shows how the depocentres and the coastline change with time as a result of the combined effect of sea-level change and climate-driven sediment input. It is clear that sea-level change is the major control on the position of the coastline and the depocentre. Six major Holocene sea-level cycles are seen, which make the delta front move over an along-stream distance of about 200 km, twice the present distance from apex to delta front.

Deposition maxima indicate the position of the main delta body. Depocentre shifts can be very rapid: between 7000 and 6500 BP, the delta front and the depocentre prograde over more than 110 km. During rapid sea-level rise or fall, the main delta body shifts almost discontinuously over the delta plain. During longer-period, lower-amplitude cycles, progradation and retrogradation are changing more continuously.

Smaller-scale fluctuations in the net sedimentation for specific time steps are superimposed upon the sea-level signal: this is the influence of climatically controlled variations in sediment input.

### 5.2. Simulated stratigraphy

Another way of visualising the output of the process–response model is in a simulated vertical cross-section along-stream (Fig. 8). In order to interpret the section of Fig. 8 correctly, the extreme vertical exaggeration has to be taken into account. We plot the

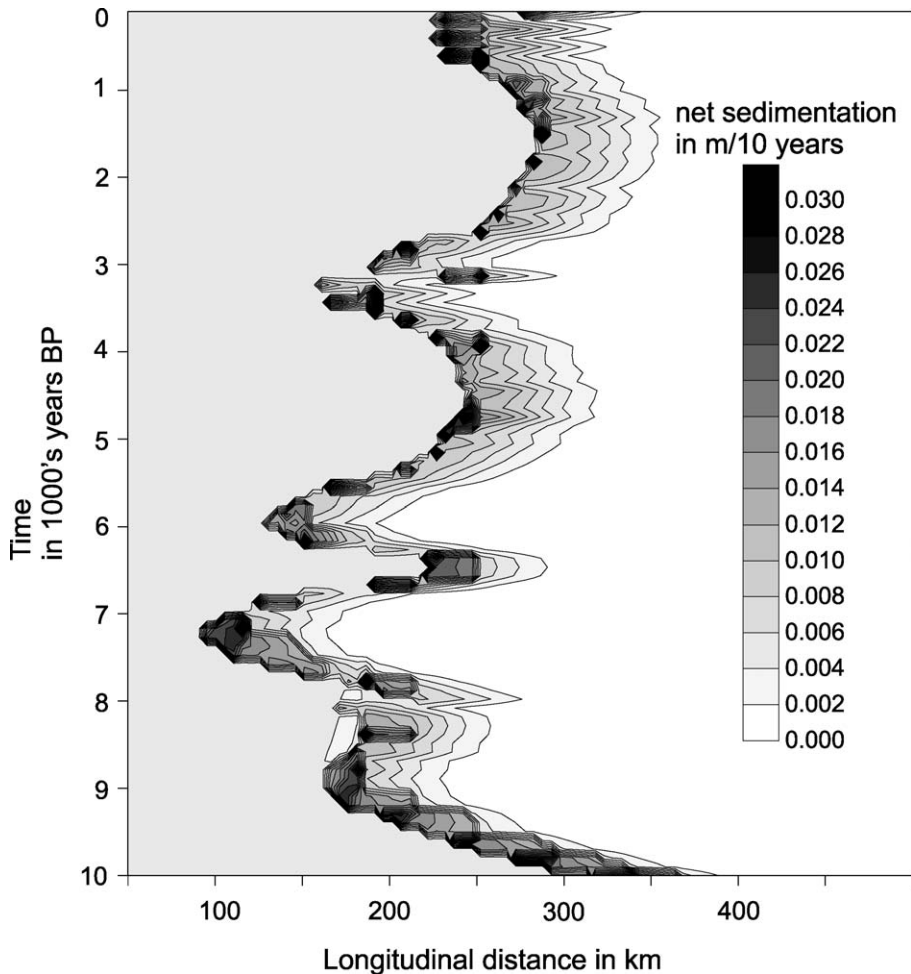


Fig. 7. Profile evolution model of the Volga delta over the Holocene. The *x*-axis shows the distance at the longitudinal profile, while the *y*-axis shows the time. Dark colors indicate the high sedimentation areas, generally, the active delta. Depocentre migration has been rapid, between 50 and 100 km migration occurred several times. Significant deposition occurred during both highstands and lowstands. Climatic fluctuations influencing sediment load and discharge over time affect the absolute yearly sedimentation rate and the extent of the deltaic plume offshore.

grain-size distribution of the layers that were deposited during simulation at certain grid cells to mimic augerings, specifically at 220–260 km, which is the area that field measurements were taken (Overeem et al., *this issue*). Two augerings taken in the field have been plotted to illustrate that similar patterns have been encountered in the field. We stress however that the different sediment layers have not been dated accurately, so that conclusive matching is impossible (Overeem et al., *this issue*). The six major sea-level cycles show up as coarsening-upwards sequences at different sites along-stream. The first transgressive

stage (TST) (1) between 10,000 and 9000 years BP is shown by a thin veneer of onlapping sequences. In the simulated pseudo-augerings, this resulted in a coarse base (Fig. 9). Delta progradation occurred at –30 m during a period of relative sea-level stability around 8000 years BP (PW1). A rapid sea-level cycle around 6000 BP resulted in a thin offlapping wedge between –24 and –26 m consisting of thin transgressive fining upwards sequence at the base and only incipient delta progradation during the short-lived highstand. In the simulated pseudo-augerings of grid cells 220, 230 and 240, it appears as a thin layer (Fig.

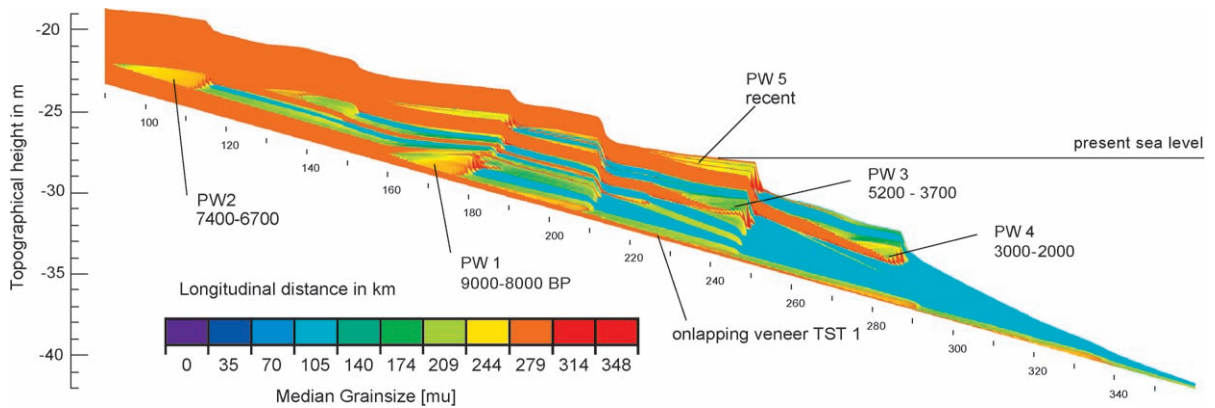


Fig. 8. Stratigraphic profile of the Volga over the Holocene based on the simulations. Thin widespread deposition results of the rapid transgression, Early Holocene. More progradational wedges (PW1–PW5) with a coarsening upward trend can be recognized at different positions along the profile.

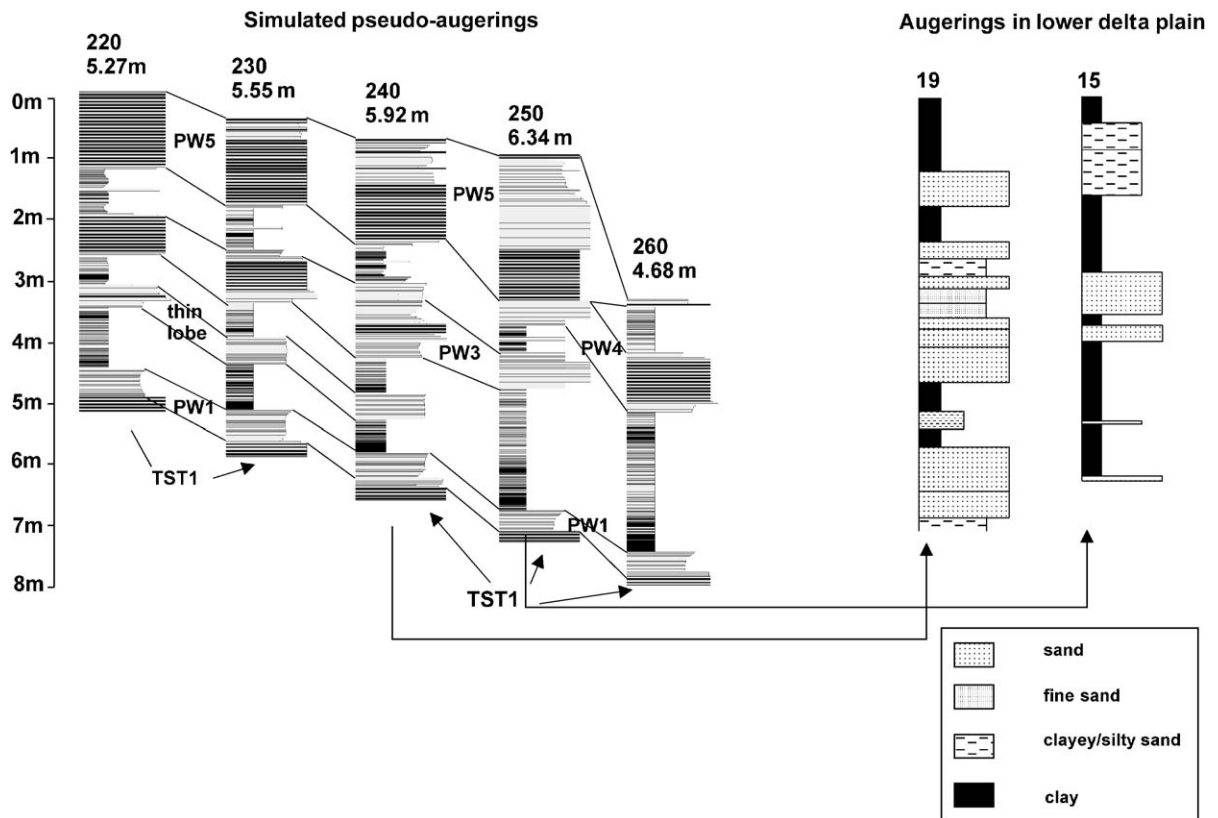


Fig. 9. Simulated augerings at 10-km interval along the longitudinal axis at positions 220–260 km, which incorporate the area that field data have been collected (as reported in accompanying paper; Overeem et al., *this issue*). Two augerings from the field area (19 and 15, located 2.5 km more downstream, Fig. 9 in Overeem et al., *this issue*) are plotted for qualitative comparison. The simulated net sedimentation, maximally 6.3 m at grid cell 250 is plausible.

9). Such a cycle could easily be mistaken for a regressive systems tract. Further basinwards, this period is represented by a condensed sequence blanketing older stages of delta progradation.

Thicker progradational wedges were produced during lowstands at  $-29$  m (5200–3700 years BP; PW 3) and  $-32$  m (2000–1000 years BP; PW 4). Smaller-scale subunits within the progradational units, as visible in the simulated augerings (Fig. 9), are largely the reflection of climate-driven variations in sediment supply. The rapid recent sea-level fluctuations (200 BP–present, PW5) had a comparably small amplitude, and an appreciable wedge has been deposited as a result. It is best developed in grid cell 250, but forms a substantial layer in all augerings (Fig. 9).

Erosion of previously deposited material occurs rarely in the model. The only example is the delta front resulting of the highstand at about 3000 years BP that is incised a little during the subsequent regression. Sequence boundaries (s.s.) are therefore not marked by unconformities or erosional hiatuses. Due to the extremely low gradient and the absence of a slope break in the initial profile, a sea-level fall is unlikely to lead to downcutting and formation of incised valley fills. Forced regression does not lead to deposition of regressional systems tracts.

As a result, the simulated stratigraphy is dominated by fining-upwards transgressional systems tracts, and coarsening-upwards progradational deltaic units,

which can occur anywhere in the profile as long as sea level remains stable for a sufficiently long period. Apparently, not all highstands produce progradational wedges, and not all lowstands produce lowstand wedges. Whether an appreciable volume of sediment is accumulating at a certain site is dependent upon the *duration* of the period of stable sea level and not on the *trend* of sea-level change. Short-lived highstands and lowstands give little signal, long-lived highstands and lowstands give well-developed sediment wedges.

Thus, when the rate of sea-level change is taken into account, periods can be selected when more significant deposition takes place. The chance that we encounter sediments in the fieldwork area, specifically deposited in those periods, would be highest. Arbitrarily, this relatively slow rate of sea-level change is taken to be 1 m/100 years (dotted line in Fig. 10) and the periods when appreciable wedges are deposited are marked. As can be seen, sediments originating from the following periods would be expected:

1. 9000–8000 years BP
2. 7400–6700 years BP
3. 5200–3700 years BP
4. 2400–900 years BP
5. the recent delta front facies

The lateral variability in this delta system is high, so that exact facies cannot be pinpointed, although

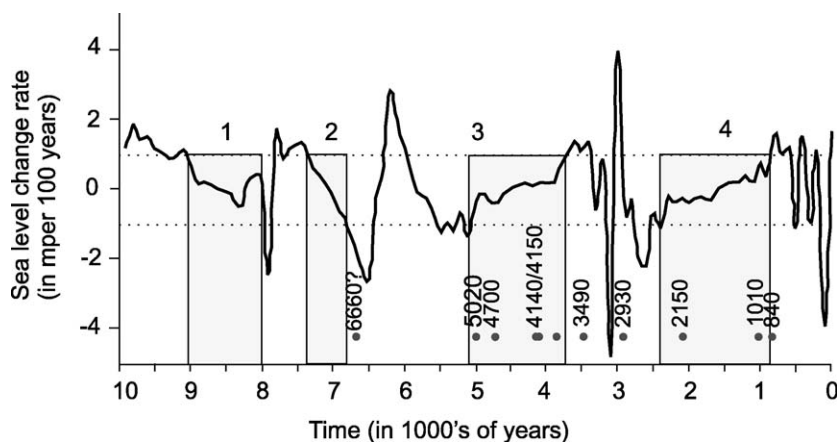


Fig. 10. Sea-level change rate over the Holocene. Arbitrarily, rates lower than 1 m/100 years (dotted line) are defined as relatively slow sea-level change. During longer periods of slow sea-level change, marked on the graph, increased localized sedimentation results in deposition of sediment wedges.  $^{14}\text{C}$  datings from the study area, plotted as small dots, provide evidence for the idea that change of encounter of sediments from these specific periods is higher.

similarities with depositional patterns found in the field can be seen (Fig. 9).

Early phase sedimentation leaves a coarse base in the simulated augerings, but conclusive evidence for remains of this phase has not been found in the study area (Overeem et al., *this issue*). Lack of datings of that age makes any identification questionable. Hypothetically, these specific lowstands (phases 1 and 2) may have been lower; the sea-level curve is inaccurate in that aspect (Rychagov, 1997). In that case, the lack of deposition becomes more plausible. Lagoonal clays and rare coeval channels, which were found in the study area (as reported in the accompanying paper; Overeem et al., *this issue*) could be linked to phase 3. The  $^{14}\text{C}$  datings corroborate this (Fig. 10). The subsequent delta front deposits in the augerings can be attributed to phase 4. Again, the  $^{14}\text{C}$  datings indicate that sediments of this period have been preserved. The deposits over the last 200 years have been clearly distinguished in the field-augerings.

## 6. Discussion and conclusions

The overall picture that emerges is that the Volga fluvio-deltaic system is entirely dominated by its low gradient; the present morphology, the migration of the depocentre under influence of sea-level changes, the limited capacity to erode and rework are all related to that single factor.

The rate of sea-level change over the Holocene has been high. Theoretically, the time scale ( $10^4$  years) is even below the fifth-order cycles used in sequence stratigraphy ( $10^4$ – $2 \times 10^6$  years), but the magnitude of the fluctuations (upto 18 m) is significant.

As a result of sea-level change and the low gradient, the depocentre shifts over the Caspian plain. The shifts were found up to 200 km over the Holocene, during the last 90 years, it amounted to 40 km. Modelling showed that in periods of these shifts mostly thin veneers of sediments are deposited. Augerings in the present delta front and lower delta plain show that several phases of rapidly alternating sedimentation occurred over the Holocene. Accurate dating of different sequences proved difficult, datable organic matter was too rarely found (Overeem et al., *this issue*).

Numerical modelling also showed that the most significant periods of deposition correlate with low

sea-level change rates, because during these periods, migration distances of the depocentre are low. Under these conditions, the most evident prograding wedges have been deposited. Remarkably, they are not necessarily correlated with sea-level falls as often assumed in classic sequence stratigraphy (Posamentier and Vail, 1988).

Furthermore, simulation showed no significant erosion despite rapid sea-level fall, so that regression does not necessarily lead to the formation of incised valleys or sequence boundaries. Schumm (1993) and Leeder and Stewart (1996) describe this case; sea level drops, but the gradient remains similar because the shelf edge is never reached. However, the classic sequence-stratigraphic concepts and laboratory experiments (Wood et al., 1993) do fail to take into account the low-gradient ramp-marginal setting, of which the Volga system is a typical example.

The process–response model, AQUATELLUS, gives plausible results when compared to field data. As such, it may be used to further explore the effects of different controlling factors in these settings. Obviously, simulations yield only a simplified situation sketch. Partly this is because we use ‘metaphysics’ for process descriptions. In addition, it is largely due to the fact that the system is only simulated in 2-D. For example, Schumm (1993) indicated the potential adjustment of a river pattern to a change in base level. The 2-D model does not allow investigation of such a mechanism. All lateral dynamics in the system are excluded. This applies for the scale of the entire delta system, where lobe switching forces locally periods of starvation. However, it applies on the local scale as well, in the fluvial system, locally fine-grained overbank sediment coexists with coarse-grained channels. In the simulation fluvial transport is rather efficient, leaving and depositing relatively coarse sediments. The effect of this simplification is that the fining and coarsening trends indicated by simulation cannot be translated directly to augerings in which a highly laterally variability in facies is encountered. The lateral variability is of such importance that the small-scale sequence grain-size trends are much more complicated than what the 2-D model indicates.

We consider the Volga system an excellent example of a low-gradient fluvio-deltaic setting. The high-frequency sea-level changes have extraordinarily impact on the location of the depocentre in time,

which may give new perspective to the ongoing discussion of the impact of sea-level fluctuations on the 'upstream' part of the fluvial system (Blum and Törnqvist, 2000). It seems that the periods of low depocentre migration distance have major impact. Major flooding surfaces or erosional surfaces are hardly developed due to the minor impact of reworking and erosion. Established large-scale sequence-stratigraphic concepts cannot be automatically scaled down because the system is almost entirely fluvial dominated and due to its low gradient.

### Acknowledgements

An initial version of the numerical model has been developed at Wageningen University by J.J. van Dijke. At Delft University of Technology, J. Storms and C. Geel shared code and ideas which further improved the present model. We thank SG reviewers A. Miall, G. Morozova and S. Bentley for their helpful suggestions.

### References

- Albertson, M.L., Yai, Y.B., Jensen, R.A., Hunter, R., 1950. Diffusion of submerged jets. *Transactions of the American Society of Civil Engineers* 115, 639–697.
- Baldina, E.A., de Leeuw, J., Gorbunov, A.K., Labutina, I.A., Zhi-vogliad, A.F., Kooistra, J.F., 1999. Vegetation change in AS-TRAKHANSKIY Biosphere Reserve (Lower Volga delta, Russia) in relation to Caspian Sea level fluctuation. *Environmental Conservation* 26 (3), 169–178.
- Belevich, E.F., 1960. About the vertical growth of islands in the lower zones of the Volga delta. *Reports Oceanogr. Comm. Ac. Sci. USSR* 6, 55–65 (in Russian).
- Blum, M.D., Törnqvist, T.E., 2000. Fluvial responses to climate and sea-level change: a review and look forward. *Sedimentology* 47 (1), 2–48.
- Bursik, M.I., 1995. Theory of the sedimentation of suspended particles from fluvial plumes. *Sedimentology* 42, 831–838.
- Coleman, J.M., Wright, L.D., 1975. Modern river deltas; variability of processes and sand bodies. In: Broussard, M. (Ed.), *Deltas; Models for Exploration*. Houston Geological Society, Houston, pp. 99–149.
- Cross, T.A., 1989. *Quantitative Dynamic Stratigraphy*. Prentice-Hall, Englewood Cliffs, 625 pp.
- den Bezemer, T., 1998. Numerical modelling of fault-related sedimentation. PhD thesis, Free University of Amsterdam, The Netherlands.
- Flemings, P.B., Grotzinger, J.P., 1996. STRATA: freeware for analyzing classic stratigraphic problems. *GSA Today* 6 (12), 1–7 publication of the Geological Society of America.
- Howes, S., Anderson, M.G., 1988. Computer simulation in geomorphology. In: Anderson, M.G. (Ed.), *Modelling Geomorphological Systems*. Wiley, Great Britain, pp. 421–440.
- Imran, J., Syvitski, J.P.M., 2000. Impact of extreme river events on the coastal ocean. *Oceanography* 13 (3), 85–92.
- Kaufman, P., Grotzinger, J.P., McCormick, D.S., 1992. A depth dependent diffusion algorithm for simulation of sedimentation in shallow marine depositional system. In: Franseen, E.K., Watney, W.L., Kendall, C.G.St.C. (Eds.), *Sedimentary Modelling; Computer Simulations and Methods for Improved Parameter Definition*. Special Publication—Kansas Geological Survey, pp. 489–508.
- Khotinskiy, N.A., 1984. Holocene climate change. In: Velichko, A.A. (Ed.), *Late Quaternary Environments of the Soviet Union*. University of Minnesota Press, Minneapolis, pp. 179–200.
- Kirkby, M.J., 1992. An erosion-limited hillslope evolution model. *Catena Supplement* 23, 157–187.
- Kooi, H., Beaumont, C., 1996. Large-scale geomorphology: classical concepts reconciled and integrated with contemporary ideas via a surface processes model. *Journal of Geophysical Research* B 101 (2), 3361–3386.
- Kosarev, A.N., Yablonskaya, E.A., 1994. *The Caspian Sea*. SPB Academic Publishing, The Hague, 259 pp.
- Kremenetski, C.V., Böttger, T., Junge, F.W., Tarasov, A.G., 1999. Late and postglacial environment of the Buzuluk area, middle Volga region, Russia. *Quaternary Science Reviews* 18, 1185–1203.
- Kroonenberg, S.B., Rusakov, G.V., Svitoch, A.A., 1997. The wandering of the Volga delta; a response to rapid Caspian sea level change. *Sedimentary Geology* 107, 189–209.
- Kroonenberg, S.B., Badyukova, E.N., Storms, J.E.A., Ignatov, E.I., Kasimov, N.S., 2000a. A full sea-level cycle in 65 years: barrier dynamics along Caspian shores. *Sedimentary Geology* 134, 257–274.
- Kroonenberg, S.B., Overeem, I., Alekseevski, N.I., Baldina, E.A., Rusakov, G.V., 2000b. Volga delta dynamics during the last 3-m sea level cycle (1929–1995). *Fluvial Archives Group Meeting Abstracts*, Mainz, March 19–24, 2000.
- Kvasov, D., 1987. The late Quaternary history of the Volga River. In: Raukas, A. (Ed.), *Paleohydrology of the Temperate Zone I; Rivers and Lakes*, pp. 43–55.
- Labutina, I.A., Baldina, E.A., Lychagin, M.Y., 1995. *Astrakhanskiy Biosphere Reserve, Damchik area. Application of GIS-techniques for the management of Astrakhanskiy Biosphere Reserve (Russia)*. Moscow State University, International Institute for Aerospace Survey and Earth Sciences (ITC) and Wageningen Agricultural University Moscow.
- Leeder, M.R., Stewart, M.D., 1996. Fluvial incision and sequence stratigraphy: alluvial responses to relative sea-level fall and their detection in the geological record. In: Hesselbo, S.P., Parkinson, D.N. (Eds.), *Sequence Stratigraphy in British Geology*. Geological Society Special Publication, vol. 103, pp. 25–39.
- Lilienberg, D.A., 1995. Current trends in the endodynamics of the Caspian Sea and changes in its water level. *Scripta Technica*, 212–218.

- Lisitzin, A.P., 1972. Sedimentation in the world oceans. SEPM Special Publication 17, 218 pp.
- Lychagin, M.Yu., Baldina, E.A., Gorbunov, A.K., Labutina, I.A., de Leeuw, J., Kasimov, N.S., Gennadiyev, A.N., Krivonosov, G.A., Kroonenberg, S.B., 1995. The Astrakhanski biosphere reserve GIS: Part 1. Present status and perspectives. *ITC Journal* 3, 189–192.
- Miall, A.D., 1991. Stratigraphic sequences and their chronostratigraphic correlation. *Journal of Sedimentary Petrology* 61, 497–505.
- Miall, A.D., 1996. *The Geology of Fluvial Deposits: Sedimentary Facies, Basin Analysis and Petroleum Geology*. Springer-Verlag, Berlin, 582 pp.
- Milliman, J.D., Syvitski, J.P.M., 1992. Geomorphic/tectonic control of sediment discharge to the ocean; the importance of small mountainous rivers. *Journal of Geology* 100, 525–544.
- Morehead, M.D., Syvitski, J.P., 1999. River plume sedimentation modeling for sequence stratigraphy: application to the Eel Margin, northern California. *Marine Geology* 154, 19–41.
- Nemec, W., 1995. The dynamics of deltaic suspension plumes. In: Oti, M.N., Postma, G. (Eds.), *Geology of Deltas*. Balkema, Rotterdam, The Netherlands, pp. 31–93.
- Ohmori, H., 1991. Change in the mathematical function type describing the longitudinal profile of a river through an evolutionary process. *Journal of Geology* 99, 97–110.
- Orton, G.J., Reading, H.G., 1993. Variability of deltaic processes in terms of sediment supply, with particular emphasis on grain size. *Sedimentology* 40, 475–512.
- Overeem, I., Kroonenberg, S.B., Veldkamp, A., Groenesteijn, K., Rusakov, G.V., Svitoch, A.A., 2002. Small-scale stratigraphy in a large ramp delta: recent and Holocene sedimentation in the Volga delta, Caspian Sea. *Sedimentary Geology* 159, 133–157 (this issue).
- Paola, C., 2000. Quantitative models of sedimentary basin filling. *Sedimentology* 47, 121–178.
- Polonski, V.F., Mikhaylov, V.N., Kir'yanov, S.V. (Eds.), 1998. *The Volga River mouth area: hydrological–morphological processes, regime of contaminants and influence of Caspian Sea level changes*. GEOS. State Oceanographic Institute and Faculty of Geography of Moscow State University (in Russian), 280 pp.
- Posamentier, H.W., Vail, P.R., 1988. Eustatic controls on clastic deposition: II. Sequence and system tract models. In: Wilgus, C.K., Hastings, B.S., Kendall, C.G.St.C., Posamentier, H.W., Ross, C.A., Van Wagoner, J.C. (Eds.), *Sea-Level Changes—An Integrated Approach*. SEPM Special Publication, vol. 42, pp. 109–124.
- Rivenaes, J.C., 1992. Application of a dual lithology, depth-dependent diffusion equation in stratigraphic simulation. *Basin Research* 4, 133–146.
- Roberts, H.H., 1998. Delta switching: early responses to the Atchafalaya river diversion. *Journal of Coastal Research* 14, 882–899.
- Rodionov, S.G., 1994. *Global and Regional Climate Interaction: The Caspian Sea Experience*. Kluwer Academic Publishing, Dordrecht, 241 pp.
- Rychagov, G.I., 1993. The sea-level regime of the Caspian Sea during the last 10,000 years. *Bulletin of the Moscow State University* 5 (2), 38–49.
- Rychagov, G.I., 1997. Holocene oscillations of the Caspian Sea, the forecasts based on palaeogeographical reconstructions. *Quaternary International* 41–42 (1), 167–172.
- Schumm, S.A., 1991. *To Interpret the Earth. Ten Ways to be Wrong*. Cambridge Univ. Press, Cambridge, 133 pp.
- Schumm, S.A., 1993. River response to baselevel change: implications for sequence stratigraphy. *Journal of Geology* 101, 279–294.
- Shanley, K.W., McCabe, P.J., 1994. Perspectives of the sequence stratigraphy of continental strata. *AAPG Bulletin* 78, 544–568.
- Sommerfield, C.K., Nittrouer, C.A., 1999. Modern accumulation rates and a sediment budget for the Eel shelf: a flood-dominated depositional environment. *Marine Geology* 154, 227–241.
- Steckler, M.S., Reynolds, D.J., Coakley, B.J., Swift, B.A., Jarrard, R.D., 1993. Modeling passive margin sequence stratigraphy. In: Posamentier, H.W., Summerhayes, C.P., Haq, B.U., Allen, G.P. (Eds.), *Sequence Stratigraphy and Facies Associations*. International Association of Sedimentologists Special Publication, vol. 18, pp. 19–41.
- Storms, J.E.A., Weltje, G.J., Van Dijke, J.J., Geel, C.R., Kroonenberg, S.B., 2002. Process–response modeling of wave-dominated coastal systems: simulating evolution and stratigraphy on geological timescales. *Journal of Sedimentary Research* 72 (2), 226–239.
- Stuiver, M., Grootes, P.M., Braziunas, T.F., 1995. The GISP2 180 climate record of the past 16,500 years and the role of the sun, ocean and volcanoes. *Quaternary Research* 44, 341–354.
- Syvitski, J.P.M., Morehead, M.D., 1999. Estimating river-sediment discharge to the ocean: application to the Eel margin, northern California. *Marine Geology* 154, 13–28.
- Tebbens, L.A., Veldkamp, A., 2000. Exploring the possibilities and limitations of modelling Quaternary fluvial dynamics. In: Maddy, D., et al. (Ed.), *River Basin Sediment Systems: Archives of Environmental Change*. Balkema, The Netherlands.
- Tebbens, L.A., Veldkamp, A., van Dijke, J.J., School, J.M., 2000. Modelling longitudinal-profile development in response to Late Quaternary tectonics, climate and sea-level changes; the River Meuse. *Global and Planetary Change* 27 (1–4), 165–186.
- Tucker, G.E., Slingerland, R.L., 1994. Erosional dynamics, flexural isostasy and long-lived escarpments; a numerical modelling study. *Journal of Geophysical Research* B 99 (6), 12229–12243.
- Vail, P.R., Mitchum Jr., R.M., Todd, R.G., Widmier, J.M., Thompson, S., Sangree, J.B., Bub, J.N., Hattelid, W.G. 1977. Seismic stratigraphy and global changes of sea-level. In: Payton, C.E. (Ed.), *Seismic Stratigraphy—Applications to Hydrocarbon Exploration*. AAPG Memoir, vol. 26, pp. 49–212.
- Veldkamp, A., van Dijke, J.J., 1998. Modeling long-term erosion and sedimentation processes in fluvial systems; a case study for the Allier–Loire system. In: Benito, G., Baker, V.R., Gregory, K.J. (Eds.), *Paleohydrology and Environmental Change*. Wiley, Chichester, pp. 53–66.
- Veldkamp, A., van Dijke, J.J., 2000. Simulating internal and external controls on fluvial terrace stratigraphy: qualitative comparison with the Maas record. *Geomorphology* 33, 225–236.
- Watney, W.L., Rankey, E.C., Harbaugh, J.W., 1999. Perspectives on stratigraphic simulation models: current approaches and future opportunities. In: Harbaugh, J.W., Watney, W.L., Rankey, E.C.,



- Wright, L.D., Goldstein, R.H., Franseen, E.K. (Eds.), Numerical Experiments in Stratigraphy: Recent Advances in Stratigraphic and Sedimentological Computer Simulations. SEPM Special publication, vol. 62, pp. 1–21.
- Winkels, H.J., Tarusova, O., Lychagin, M.Y., Rusakov, G.J., Kasimov, N.S., Kroonenberg, S.B., Marin, G., van Munster, G., 1996. Geochronology of priority pollutants in sedimentation zones of the Volga Delta, in comparison with the Rhine and Danube Delta. Riza nota no: 96.078 Institute of Inland Water Management and Wastewater Treatment, The Netherlands.
- Wood, L.J., Ethridge, F.G., Schumm, S.A., 1993. The effects of rate of base-level fluctuation on coastal-plain, shelf and slope systems: an experimental approach. In: Posamentier, H.W., Summerhayes, C.P., Haq, B.U., Allen, G.P. (Eds.), Sequence Stratigraphy and Facies Associations. IAS Special Publication, vol. 18, pp. 43–53.
- Wright, L.D., 1977. Sediment transport and deposition at river mouths; a synthesis. Geological Society of America Bulletin 88, 857–868.